

# Towards a mechanism of AMP-substrate inhibition in adenylate kinase from *Escherichia coli*

Michael A. Sinev<sup>a,b</sup>, Elena V. Sineva<sup>a</sup>, Varda Ittah<sup>a</sup>, Elisha Haas<sup>a,\*</sup>

<sup>a</sup>Department of Life Sciences, Bar-Ilan University, Ramat Gan 52900, Israel

<sup>b</sup>Institute of Biochemistry and Physiology of Microorganisms, Russian Academy of Sciences, 142292 Pushchino (Moscow Region), Russia

Received 30 August 1996; revised version received 10 October 1996

**Abstract** Crystallographic studies on adenylate kinase (AK) suggest that binding of ATP causes the LID domain of the enzyme to close over the ATP molecule (Schlauderer et al. (1996) *J. Mol. Biol.* 256, 223–227). The method of time-resolved fluorescence resonance energy transfer was applied to study the proposed structural change in AK from *Escherichia coli*. Two active derivatives of the (C77S, A73C, V142C)-AK mutant containing the excitation energy donor attached to one of the two cysteine residues and the acceptor attached to the other cysteine were prepared to monitor displacements of the LID domain in response to substrate binding. Binding of either ATP or AMP was accompanied by a  $\sim 9$  Å decrease in the interprobe distances suggesting LID domain closure. Closure of the LID domain in response to AMP binding may be a possible reason for the strong AMP-substrate inhibition known for *E. coli* AK.

**Key words:** Adenylate kinase; Site-directed mutagenesis; Time-resolved fluorescence; Energy transfer; Probe; Substrate inhibition

## 1. Introduction

Adenylate kinase (AK) from *Escherichia coli* belongs to a family of small monomeric enzymes catalyzing the phosphoryl transfer reaction ( $\text{MgATP} + \text{AMP} \leftrightarrow \text{MgADP} + \text{ADP}$  [1]). The enzyme consists of the CORE domain (residues 1–29, 60–119, 158–214) and two small domains, the AMP-binding (AMP<sub>bind</sub>) domain (residues 30–59) and the LID domain (residues 120–159) [2]. Availability of the crystal structures for AKs in the presence of different ligands, and high structural similarity found within the AK family, has enabled the deduction of a relatively detailed model of the structural transitions of the enzyme during catalysis [3]. This model suggests that formation of the AK·AMP binary complex is followed by closure of the AMP<sub>bind</sub> domain over the AMP molecule, while the position of the LID domain remains unchanged and the ATP-binding site is not blocked [4,5]. Formation of the AK·ATP binary complex is followed by closure of the LID domain of the enzyme over the ATP molecule, while the AMP<sub>bind</sub> domain remains unclosed [6]. Thus, crystallographic studies on AKs suggest independent closure of the small domains of the enzyme following the formation of the ternary enzyme–substrate complex.

To analyze domain closure in AK, we produced a number of two-cysteine-containing mutants of the *E. coli* enzyme, having cysteine residues in the expected movable segments of the enzyme molecule. These mutants, labeled with the appropriate donor and acceptor fluorescent probes are being used to study

structural transitions of the enzyme by the method of fluorescence resonance energy transfer (ET). The data we recently obtained strongly support the proposed structural transitions in AK and suggest the closure of the AMP<sub>bind</sub> domain in response to AMP binding [7]. Here we report the evidence for the closure of the LID domain of the enzyme in response to ATP binding.

## 2. Materials and methods

### 2.1. Preparation of labeled derivatives

Recombinant plasmids coding for (C77S, A73C)-AK (C<sub>73</sub>-AK), (C77S, V142C)-AK (C<sub>142</sub>-AK) and (C77S, A73C, V142C)-AK (C<sub>73</sub>C<sub>142</sub>-AK) mutants were prepared by the site-directed mutagenesis method described by Kunkel et al. [8]. Mutants were purified as previously described [7] and checked for the presence of cysteine residues by the Ellman reaction [9]. Labeling of single-cysteine C<sub>73</sub>- and C<sub>142</sub>-AK mutants with 5-iodoacetamidosalicylic acid (the donor, D) or 5-iodoacetamidofluorescein (the acceptor, A) was performed in 0.1 M Tris-HCl (pH 8.0) at a high dye-to-protein molar ratio (10:20). The labeled AK derivatives (D<sub>73</sub>-AK, D<sub>142</sub>-AK, A<sub>73</sub>-AK or A<sub>142</sub>-AK) were separated from the unlabeled mutants by anion exchange chromatography (see Fig. 1A–D). The double-labeled AK derivative, A<sub>73</sub>D<sub>142</sub>-AK, containing the donor probe attached to Cys-142 and the acceptor probe attached to Cys-73, was prepared by a two-step labeling procedure. C<sub>73</sub>C<sub>142</sub>-AK was first reacted with an equimolar amount of 5-iodoacetamidosalicylic acid. After the reaction a mixture of AK derivatives containing C<sub>73</sub>C<sub>142</sub>-AK, C<sub>73</sub>D<sub>142</sub>-AK, D<sub>73</sub>C<sub>142</sub>-AK and D<sub>73</sub>D<sub>142</sub>-AK was separated by anion exchange chromatography (see Fig. 1E). The C<sub>73</sub>D<sub>142</sub>-AK derivative was further reacted with 5-iodoacetamidofluorescein, and the double-labeled A<sub>73</sub>D<sub>142</sub>-AK derivative was purified from the acceptor-unlabeled derivative (Fig. 1F). The D<sub>73</sub>A<sub>142</sub>-AK derivative was prepared using a similar procedure.

The kinetic constants ( $K_m$  and  $V_{max}$ ) for AK derivatives were measured in the direction of ADP formation as described previously [7]. The concentration of protein solutions for the labeled AK derivatives was determined by the method of Lowry et al. [10] using wild-type AK as a calibration standard. The protein concentration for wild-type AK was determined by using the absorption coefficient  $A_{277nm} = 0.5$  (mg/ml)<sup>-1</sup> cm<sup>-1</sup> [11].

### 2.2. Time-resolved energy transfer measurements

Decay of the donor emission was measured at 20°C using the time-correlated single-photon counting system described previously [12]. Donor emission was excited at 310 nm and monitored at 435 nm (bandwidth, 12 nm). Each set of ET experiments included measurements of two protein samples (e.g., D<sub>73</sub>-AK and D<sub>73</sub>A<sub>142</sub>-AK) prepared in 0.1 M Tris-HCl (pH 7.5) containing the same protein concentration (0.1 mg/ml) and the same ligand concentration. Efficiency of ET ( $E$ ) was calculated from the average lifetimes of the donor,  $\langle\tau_d\rangle$  and  $\langle\tau_{da}\rangle$ , in the absence and in the presence of the acceptor:  $E = 1 - \langle\tau_{da}\rangle / \langle\tau_d\rangle$ . The average lifetime of the donor was determined from multiexponential analysis of the donor emission decay:  $\langle\tau\rangle = \sum_i \alpha_i \tau_i$ , where  $\alpha_i$  and  $\tau_i$  are the relative amplitude ( $\sum_i \alpha_i = 1$ ) and the lifetime of the  $i$ th decay component, respectively. Average interprobe distances ( $R$ ) in the D<sub>73</sub>A<sub>142</sub>-AK and the A<sub>73</sub>D<sub>142</sub>-AK derivatives were calculated from the respective  $E$  values [13,14]:

$$R = R_0(1/E - 1)^{1/6}; \quad R_0 = (8.79 \times 10^{-5} \kappa^2 n^{-4} Q_d J_{da})^{1/6}$$

\*Corresponding author. Fax: (972) 3-535-1824.  
E-mail: haas@brosh.cc.biu.ac.il

where  $R_0$  is the Förster distance (in Å);  $\kappa^2$  is the orientation factor (taken as 2/3);  $n$  is the refractive index of the medium between the donor and acceptor (taken as 1.34);  $Q_d$  is the quantum yield of the donor in the absence of the acceptor; and  $J_{da}$  is the normalized spectral overlap integral (in  $M^{-1} cm^{-1} nm^4$ ). The overlap integral,  $J_{da} = \int f_d(\lambda)\epsilon_a(\lambda)\lambda^4 d\lambda / \int f_d(\lambda)d\lambda$ , was calculated using the fluorescence emission spectrum of the donor in  $D_{73}$ -AK (or  $D_{142}$ -AK),  $f_d(\lambda)$ , and the absorption spectrum of the acceptor in  $A_{142}$ -AK (or  $A_{73}$ -AK),  $\epsilon_a(\lambda)$ , measured under the respective ligand conditions. Quantum yield of the donor was measured relative to that of quinine sulfate (taken to be 0.55 [15]). The values of  $Q_d$  in the  $D_{142}$ -AK and in the  $D_{73}$ -AK derivatives in the absence of ligands were 0.28 and 0.33, respectively.

### 3. Results and discussion

To monitor displacements of the LID domain in AK, double-labeled derivatives of the (C77S, A73C, V142C)-AK mutant of the *E. coli* enzyme containing one of the fluorescent probes attached to Cys-142 in the LID domain and the other attached to Cys-73 in the CORE domain were prepared. Both  $A_{73}D_{142}$ -AK and  $D_{73}A_{142}$ -AK derivatives were highly active (Table 1) and revealed the strong AMP-substrate inhibition which is a characteristic feature of wild-type AK (Fig. 2). The Förster distances ( $R_0$ s) calculated for these two derivatives in the absence of ligands were 38.3 and 39.4 Å, respectively. The absorption spectra of both the donor and the acceptor probes were independent of the labeling site (examples are presented in Fig. 3). The ligands studied (AMP, ATP and bi-substrate analogue inhibitor  $P^1, P^5$ -di(adenosine-5')pentaphosphate [AP<sub>5</sub>A]) affect neither the position of the fluorescence spectrum of the donor (in  $D_{73}$ -AK and  $D_{142}$ -AK) nor the absorption spectrum of the acceptor (in  $A_{73}$ -AK and  $A_{142}$ -AK).  $R_0$  values corresponding to the different ligand conditions were practically the same as those in the absence of ligands.

Both the steady-state and the time-resolved ET experiments were performed for each of the double-labeled derivatives. The steady-state ET experiments included measurements of the fluorescence emission spectra of  $D_{142}$ -,  $A_{73}D_{142}$ - and  $A_{73}$ -AK (and of  $D_{73}$ -,  $D_{73}A_{142}$ - and  $A_{142}$ -AK) and the spectra of the same derivatives in the presence of AMP (10 mM), ATP (20 mM), MgATP (20 mM) and AP<sub>5</sub>A (1 mM) (as an example, see Fig. 4). (It should be noted that these ligand concentrations were high enough to produce a fully saturated enzyme [7].) These measurements served both as an indication of the appropriate conditions for further time-resolved ET experiments, and as an independent control for the ET. From Fig. 4 it is clear that the yield of the donor emission was reduced in the presence of the acceptor in  $A_{73}D_{142}$ -AK while the yield of the acceptor emission was increased. This is a clear demonstration of ET between the donor and the acceptor probes in the DA-AK derivatives. Multiexponential analysis of the donor emission decay in the  $D_{142}$ -AK and

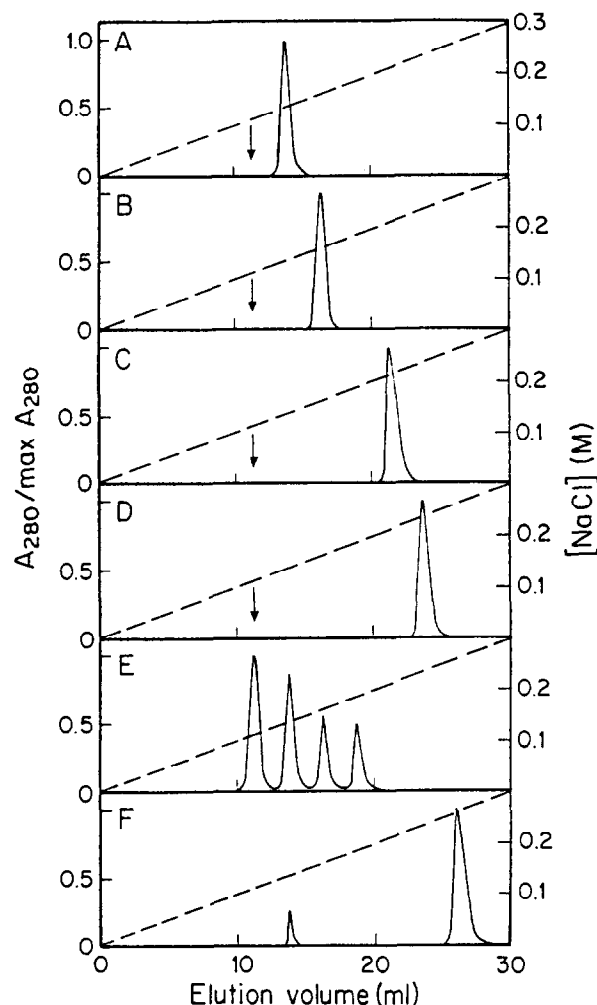


Fig. 1. Separation of AK derivatives by anion exchange chromatography on Mono Q column (FPLC). Elution profiles of  $D_{142}$ -AK (A),  $D_{73}$ -AK (B),  $A_{142}$ -AK (C),  $A_{73}$ -AK (D), two-cysteine-containing  $C_{73}C_{142}$ -AK mutant after the reaction with an equimolar amount of 5-iodoacetamidofluorescein (E), and  $C_{73}D_{142}$ -AK after the reaction with 5-iodoacetamidofluorescein (F) are shown. 150  $\mu$ l of each protein solution (1–1.5 mg/ml) in 20 mM Tris-HCl (pH 8.0) were applied to a Mono Q column (0.5  $\times$  5 cm) equilibrated with the same buffer. The column was washed by 5 ml of the buffer and the proteins were eluted with a linear gradient of NaCl (0–0.3 M) in 30 ml of the buffer at a flow rate of 0.5 ml/min. The arrow in panels A–D marks the elution volume value corresponding to the peak position of the unlabeled  $C_{73}$ -,  $C_{142}$ -,  $C_{73}C_{142}$ -AK mutants and wild-type AK. The four peaks shown in panel E correspond (from left to right) to  $C_{73}C_{142}$ -AK,  $C_{73}D_{142}$ -AK,  $D_{73}C_{142}$ -AK and  $D_{73}D_{142}$ -AK. The minor and major peaks shown in panel F correspond to  $C_{73}D_{142}$ -AK and  $A_{73}D_{142}$ -AK, respectively.

Table 1  
Apparent kinetic constants of wild-type AK, (C77S, A73C, V142C)-AK mutant and its double-labeled derivatives

Enzyme	ATP (as variable substrate <sup>a</sup> )		AMP (as variable substrate <sup>b</sup> )	
	$K_m$ ( $\mu$ M)	$V_{max}$ (IU/mg)	$K_m$ ( $\mu$ M)	$V_{max}$ (IU/mg)
Wild-type AK	144 $\pm$ 4	1050 $\pm$ 40	33 $\pm$ 2	1038 $\pm$ 50
(C77S, A73C, V142C)-AK	133 $\pm$ 4	1040 $\pm$ 40	34 $\pm$ 4	982 $\pm$ 70
$D_{73}A_{142}$ -AK	111 $\pm$ 8	557 $\pm$ 30	24 $\pm$ 2	633 $\pm$ 30
$A_{73}D_{142}$ -AK	163 $\pm$ 6	943 $\pm$ 50	43 $\pm$ 4	1046 $\pm$ 60

Kinetic constants were measured at 25°C in 0.1 M Tris-HCl (pH 7.5) containing 0.1 M KCl.

<sup>a,b</sup>Concentrations of fixed substrates: 0.2 mM AMP (<sup>a</sup>) and 1 mM ATP (<sup>b</sup>).

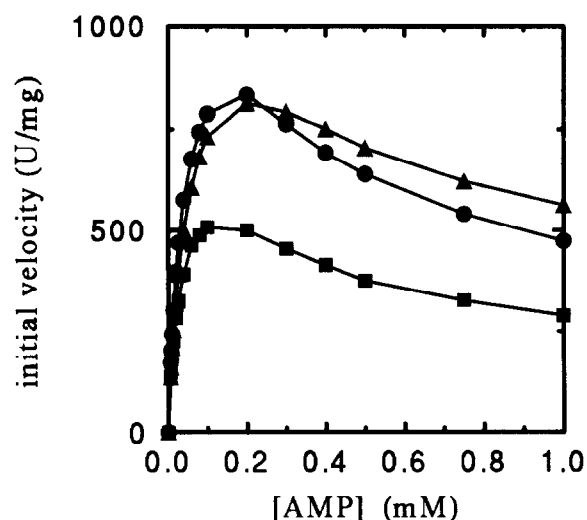


Fig. 2. AMP substrate inhibition for wild-type AK (●),  $D_{73}A_{142}$ -AK derivative (■) and  $A_{73}D_{142}$ -AK derivative (▲). Initial velocities of AK reaction were measured under conditions described in Table 1.

$A_{73}D_{142}$ -AK derivatives, and ET efficiencies calculated for different ligand forms of the  $A_{73}D_{142}$ -AK derivative are presented in Table 2. Binding of ligands to  $A_{73}D_{142}$ -AK caused an increase in ET efficiency in the following order: no ligand < AMP  $\approx$  ATP  $\approx$  MgATP < AP<sub>5</sub>A. The same dependence was obtained with  $D_{73}A_{142}$ -AK. No intermolecular ET was detected: the decay of the donor emission in the equimolar mixture of D- and A-AK was the same as in the absence of the A-AK derivative.

Average interprobe distances (IPD) in different ligand forms of the double-labeled AK derivatives are presented in Table 3. For each of the ligand forms studied, IPD in  $D_{73}A_{142}$ -AK was very similar to that in  $A_{73}D_{142}$ -AK. Binding of either ATP or AMP caused a  $\sim 9$  Å decrease in IPD. Further decrease in IPD ( $\sim 3$  Å) was observed upon the formation of AK·AP<sub>5</sub>P complex. According to the proposed model of domain closure in AK [3,6], binding of ATP to *E. coli* AK causes closure of the LID domain of the enzyme, which is followed by a  $\sim 10$  Å decrease in the  $C_{\alpha}(73)$ – $C_{\alpha}(142)$  distance (see the last column of Table 3). Formation

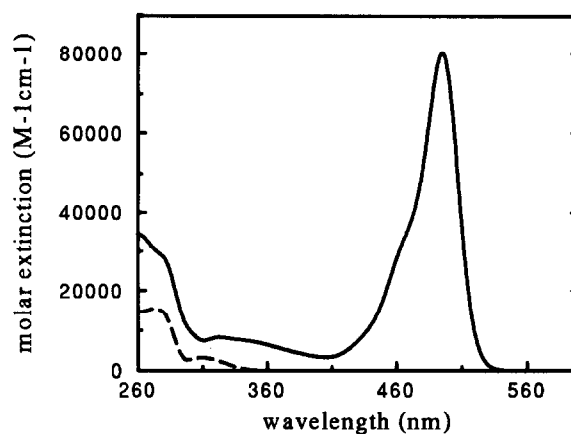


Fig. 3. Absorption spectra of  $D_{142}$ -AK (---) and  $A_{73}$ -AK (—) in 0.1 M Tris-HCl (pH 7.5). The absorption spectra of  $D_{73}$ -AK and  $A_{142}$ -AK (not shown) are almost identical to those of  $D_{142}$ -AK and  $A_{73}$ -AK, respectively.

of the AK·AP<sub>5</sub>P ‘ternary’ complex causes a further closure of the LID domain, which is followed by a further 3–4 Å decrease in the  $C_{\alpha}(73)$ – $C_{\alpha}(142)$  distance. Thus, the data obtained strongly support the proposed closure of the LID domain of AK in response to ATP (or AP<sub>5</sub>P) binding. Furthermore, our data suggest that AMP binding causes closure of the LID domain of AK to approximately the same extent as does ATP binding.

The mechanisms underlying the strong AMP-substrate inhibition in *E. coli* AK is a subject of much discussion [18–21]. Two opposing models were reported to explain the phenomenon. The first of these is a competitive inhibition model, which suggests that AMP possesses a relatively high affinity towards the ATP binding site [19]. The second model fails to address this possibility, and considers the inhibition to be of a pure uncompetitive type [20]. Up to now there is no convincing evidence for one or other of these models. However, it is known that *E. coli* AK does not show clear competitive inhibition [18,20]. Direct binding studies revealed only one binding site for AMP [11] in the wild-type enzyme. Furthermore, crystallographic studies on *E. coli* AK complexed with both AMP and the ATP analogue molecules showed that AMP occupies only its own binding site (no AMP was found bound

Table 2  
Multiexponential analysis of the time-resolved fluorescence of the donor in  $D_{142}$ - and  $A_{73}D_{142}$ -AK derivatives under different ligand conditions

Ligand	$\tau_d^a$ (ns)				$\tau_{da}^b$ (ns)				<i>E</i> (%) <sup>c</sup>
	$\tau_1$ ( $\alpha_1$ )	$\tau_2$ ( $\alpha_2$ )	$\langle \tau_d \rangle$	$\chi^2$	$\tau_1$ ( $\alpha_1$ )	$\tau_2$ ( $\alpha_2$ )	$\langle \tau_d \rangle$	$\chi^2$	
None	1.84 (0.26)	7.43 (0.74)	5.98	1.16	1.81 (0.25)	6.53 (0.75)	5.35	1.20	10.5 ± 1.3
10 mM AMP	1.76 (0.25)	7.17 (0.75)	5.82	1.28	1.89 (0.34)	5.65 (0.66)	4.37	1.57	24.9 ± 1.1
20 mM ATP	1.69 (0.26)	7.03 (0.74)	5.64	1.39	1.87 (0.40)	5.64 (0.60)	4.13	1.38	26.8 ± 1.0
20 mM MgATP	1.51 (0.28)	6.93 (0.72)	5.41	1.78	1.88 (0.41)	5.36 (0.59)	3.93	1.64	27.4 ± 1.0
1 mM AP <sub>5</sub> A	1.62 (0.25)	7.26 (0.75)	5.85	1.33	1.68 (0.37)	5.25 (0.63)	3.93	2.06	32.8 ± 1.0

Measurements of the time-resolved fluorescence of the donor were performed using 310-nm excitation. Donor emission was recorded at 435 nm. <sup>a,b</sup>Decay parameters of the donor emission in  $D_2$ -AK (<sup>b</sup>) and  $D_2A_1$ -AK (<sup>c</sup>):  $\tau_i$  and  $\alpha_i$  are the lifetime and the relative amplitude of the *i*th decay component, respectively (errors in  $\tau_i$  and  $\alpha_i$  are  $\pm 10\%$  of the presented values);  $\langle \tau_d \rangle$  and  $\langle \tau_{da} \rangle$  are the average (amplitude-weighted) lifetimes of the donor in  $D_2$ - and  $D_2A_1$ -AK, respectively (errors in the average lifetimes are  $\pm 1\%$  of the presented values).

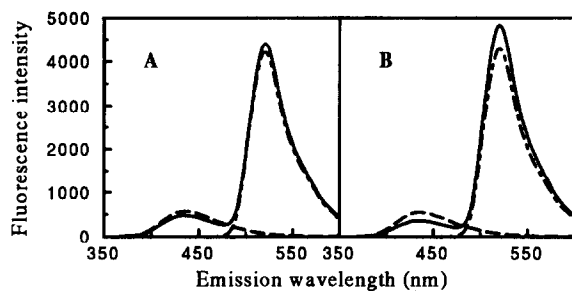


Fig. 4. Fluorescence emission spectra of  $D_{142}$ -AK (— — —),  $A_{73}D_{142}$ -AK (—) and  $A_{73}$ -AK (— — —) measured in the absence of ligands (A) and in the presence of 1 mM  $AP_5A$  (B). The wavelength of excitation was 310 nm. The bandwidths were 16 nm at both the excitation and emission monochromators. The concentration of each protein solution (prepared in 0.1 M Tris-HCl (pH 7.5)) was 0.1 mg/ml.

Table 3

Average interprobe distances in different ligand forms of  $D_{73}A_{142}$ - and  $A_{73}D_{142}$ -AK

Ligand	Interprobe distance (Å)		$R_{\text{cryst}}^a$ (Å)
	$D_{73}A_{142}$ -AK	$A_{73}D_{142}$ -AK	
None	54.5 ± 2.0	54.8 ± 2.1	51.7
AMP	45.1 ± 1.4	46.1 ± 1.5	51.6
ATP	46.9 ± 1.5	45.3 ± 1.4	41.6
$AP_5A$	42.9 ± 1.3	43.0 ± 1.3	37.3 (39.0)

<sup>a</sup>Distances between  $C_{\alpha}$  atoms of those amino acid residues structurally equivalent to residues 73 and 142 of *E. coli* AK [3], in the crystal structures of: apo-AK (for *E. coli* AK) [2], AK-AMP binary complex (for AK from beef mitochondrial matrix) [4], AK-AMPPCF<sub>2</sub>P binary complex (for the mutant enzyme of yeast AK) [6] and AK- $AP_5A$  pseudoternary complex (*E. coli* AK) [16]. The value in parentheses is the corresponding distance in the crystal structure of AK- $AP_5A$  complex for yeast AK [17].

to the ATP site) [22]. These experimental data exclude the possibility of strong affinity of AMP towards the ATP binding site.

The data we obtained here suggest that the binding of AMP causes closure of the LID domain. The closure of the LID domain in response to AMP binding can prevent further binding of ATP to the ATP binding site, resulting in uncompetitive inhibition. One question which remains unclear is whether the closure of the LID domain occurs upon the formation of the AK-AMP binary complex (when AMP binds to the AMP binding site) or upon the further formation of the AMP-AK-

AMP ternary complex (when the second AMP molecule binds to the ATP binding site). If the first is true, then the AMP inhibition is uncompetitive. If the second situation is true, the inhibition could be much stronger than in the case of pure competitive inhibition. In either case, closure of the LID domain in response to AMP binding may explain the strong AMP-substrate inhibition known for *E. coli* AK.

## References

- [1] Noda, L. (1973) in: The Enzymes (Boyer, P.D., Ed.), Vol. 8, pp. 279–305, Academic Press, New York.
- [2] Müller, C.W., Schlauderer, G.J., Reinstein, J. and Schulz, G.E. (1996) Structure 4, 147–156.
- [3] Vonrhein, C., Schlauderer, G.J. and Schulz, G.E. (1995) Structure 3, 483–490.
- [4] Deiderichs, K. and Schulz, G.E. (1991) J. Mol. Biol. 217, 541–549.
- [5] Gerstein, M., Schulz, G. and Chothia, C. (1993) J. Mol. Biol. 229, 494–501.
- [6] Schlauderer, G.J., Proba, K. and Schulz, G.E. (1996) J. Mol. Biol. 256, 223–227.
- [7] Sinev, M.A., Sineva, E.V., Ittah, V. and Haas, E. (1996) Biochemistry 35, 6425–6437.
- [8] Kunkel, T.A., Roberts, J.D. and Zakour, R.A. (1987) Methods Enzymol. 154, 367–382.
- [9] Riddles, P.W., Blakely, R.L. and Zerner, B. (1979) Anal. Biochem. 94, 75–81.
- [10] Lowry, O.H., Rosebrough, N.J., Farr, A.L. and Randall, R.J. (1951) J. Biol. Chem. 193, 265–275.
- [11] Girons, I.S., Gilles, A.-M., Margarita, D., Michelson, S., Monnot, M., Fermandjian, S., Danchin, A. and Bârză, O. (1987) J. Biol. Chem. 262, 622–629.
- [12] Gottfried, D.S. and Haas, E. (1992) Biochemistry 31, 12353–12362.
- [13] Förster, T. (1948) Ann. Phys. (Leipzig) 2, 55–75.
- [14] Fairclough, R.H. and Cantor, C.R. (1978) Methods Enzymol. 48, 347–379.
- [15] Melhuish, W.H. (1960) J. Phys. Chem. 64, 762–764.
- [16] Müller, C.W. and Schulz, G.E. (1992) J. Mol. Biol. 224, 159–177.
- [17] Abele, U. and Schulz, G.E. (1995) Protein Sci. 4, 1262–1271.
- [18] Gilles, A.-M., Marlière, P., Rose, T., Sarfati, R., Longin, R., Meier, A., Fermandjian, S., Monnot, M., Cohen, G.N. and Bârză, O. (1988) J. Biol. Chem. 263, 8204–8209.
- [19] Reinstein, J., Vetter, I.R., Schlichting, I., Rösch, P., Wittinghofer, A. and Goody, R.S. (1990) Biochemistry 29, 7440–7450.
- [20] Liang, P., Phillips, G.N., Jr. and Glaser, M. (1991) Proteins 9, 28–36.
- [21] Bilderback, T., Fulmer, T., Mantulin, W.W. and Glaser, M. (1996) Biochemistry 35, 6100–6106.
- [22] Berry, M.B., Meador, B., Bilderback, T., Liang, P., Glaser, M. and Phillips, G.N., Jr. (1994) Proteins 19, 183–198.